Electronic Supplementary Material (ESI) for Materials Horizons.
This journal is © The Royal Society of Chemistry 2023

Supporting Information

Covalent organic frameworks with flexible spacers in hybrid PEMs enable highly efficient proton conductivity

Ziwen Liu[1,2‡], Xiao Pang[1,2‡], Benbing Shi[1,2], Na Xing[1,2], Yawei Liu[3], Bohui Lyu[1,2], Leilang Zhang[1,2], Yan Kong[1,2], Sijia Wang[1,2], Zhong Gao[1,2], Rou Xue[1,2], Tianyu Jing[1,2], Changkun Liu[1,2], Huidan Baiqin[1,2], Hong Wu[1,2*] and Zhongyi Jiang[1,2,4*]

1. Key Laboratory for Green Chemical Technology of Ministry of Education, School of Chemical Engineering and Technology, Tianjin University, Tianjin 300072, China.

2. Haihe Lab Sustainable Chem Transformations, Tianjin 300192, Peoples R China

3. Beijing Key Laboratory of Ionic Liquids Clean Process, CAS Key Laboratory of Green Process and Engineering, Institute of Process Engineering, Chinese Academy of Sciences, Beijing, 100190, China.

4. Joint School of National University of Singapore and Tianjin University, International Campus of Tianjin University, Binhai New City, Fuzhou, 350207, China.

‡ These authors are co-first authors in this work.

*Correspondence to: wuhong@tju.edu.cn (Hong Wu), zhyjiang@tju.edu.cn (Zhongyi Jiang)

1 Experimental Section

Synthesis of Bd-C_3-SO_3H and Bd-C_4-SO_3H:

The synthesis procedures of 3,3'-(-4.4'-Diamino-3,3'-biphenylylenedioxy) dipropanesulfonic acid (Figure S1, Bd-C_3-SO_3H), 4,4'-(-4.4'-Diamino-3,3'-biphenylylenedioxy)dibutanesulfonic acid(Figure S2, Bd-C_4-SO_3H) were described as follows. 3,3'-Dihydroxybenzidine (1g) was dissolved by boiling with glacial acetic acid (50 mL) with the subsequent addition of water (12 mL). The solution was filtered and cooled down to room temperature. Then, the solution was heated to 50°C and acetic anhydride (50 mL) was added. The mixed solution was stirred for 36 h and the colorless solid was filtered off with subsequent washing by acetic acid for three times. Afterwards, the purified solid (4,4'-diacetamido-3,3'-dihydroxybiphenyl) was crystallized from benzyl alcohol and dried at 150°C for 12 h.

4,4'-diacetamido-3,3'-dihydroxybiphenyl (4.55g, 0.015 mol) was added to sodium hydroxide solution (NaOH: 1.32 g, 0.033 mol; methanol: 50 mL) followed by a suspension of 1,3-propanesultone (3.66g, 0.03 mol). The mixture was stirred and heated for 1 h at 85°C and then cooled to about 5°C. The precipitate was filtered off and dried at 45°C for 12 h.

The dried product (5 g, 0.0084 mol) was dissolved in water (20 mL) and passed through a cation exchange column (730). The filtrate was concentrated to about 5 mL and added to concentrated hydrochloric acid (70 mL) and refluxed for 2 h. After being cooled to room temperature, the 3,3'-(-4.4'-Diamino-3,3'-biphenylylenedioxy)dipropanesulfonic acid precipitated and was collected by filtration. An analytically pure product was obtained when this crude product was crystallized from water.

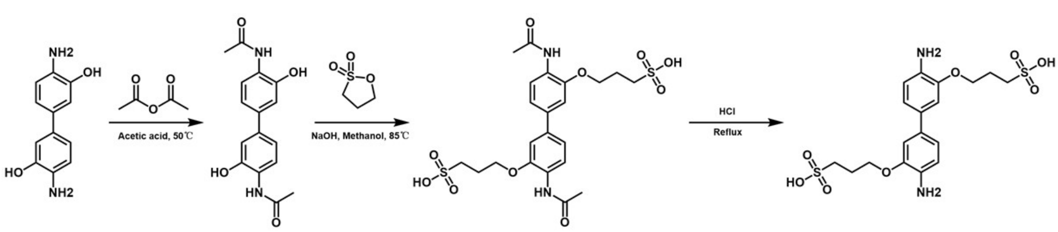

Figure S1 The synthesis of Bd-C_3-SO_3H

4,4'-(-4.4'-Diamino-3,3'-biphenylylenedioxy) dibutanesulfonic acid was prepared from 1,4-butanesultone and the synthesis procedure was followed as mentioned above.

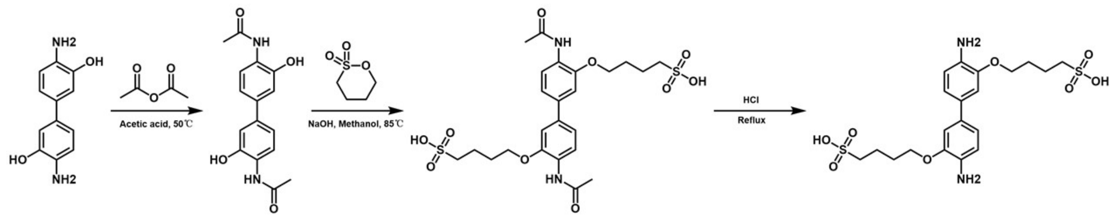

Figure S2 The synthesis of Bd-C_4-SO_3H

2 Figures and tables

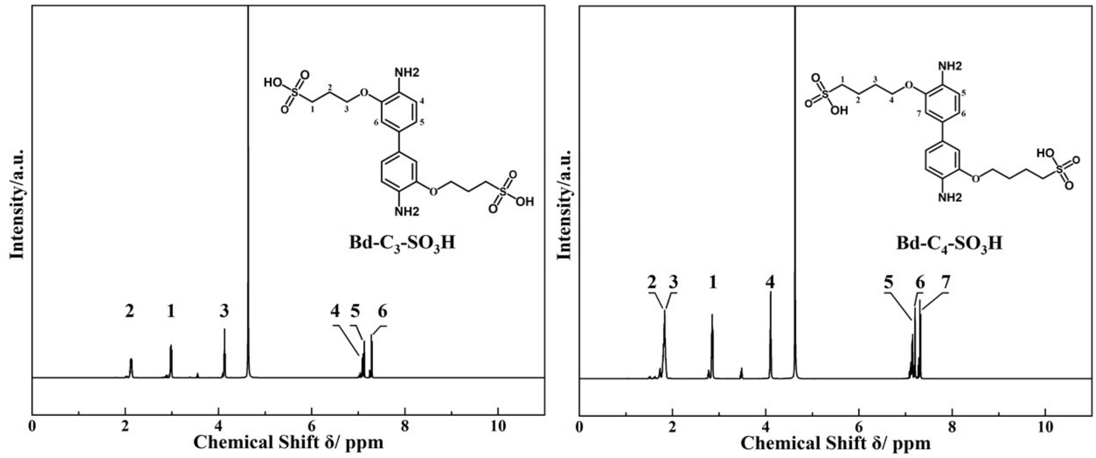

Figure S3 ^{1}H-NMR spectra of the Bd-C_3-SO_3H and Bd-C_4-SO_3H

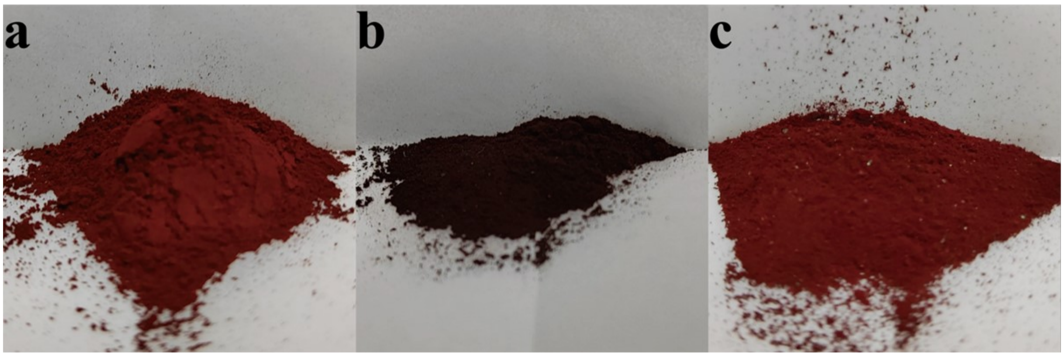

Figure S4 Digital photos of iCOF powders

(a) TpBd-SO_3H; (b) TpBd-C_3-SO_3H; (c) TpBd-C_4-SO_3H

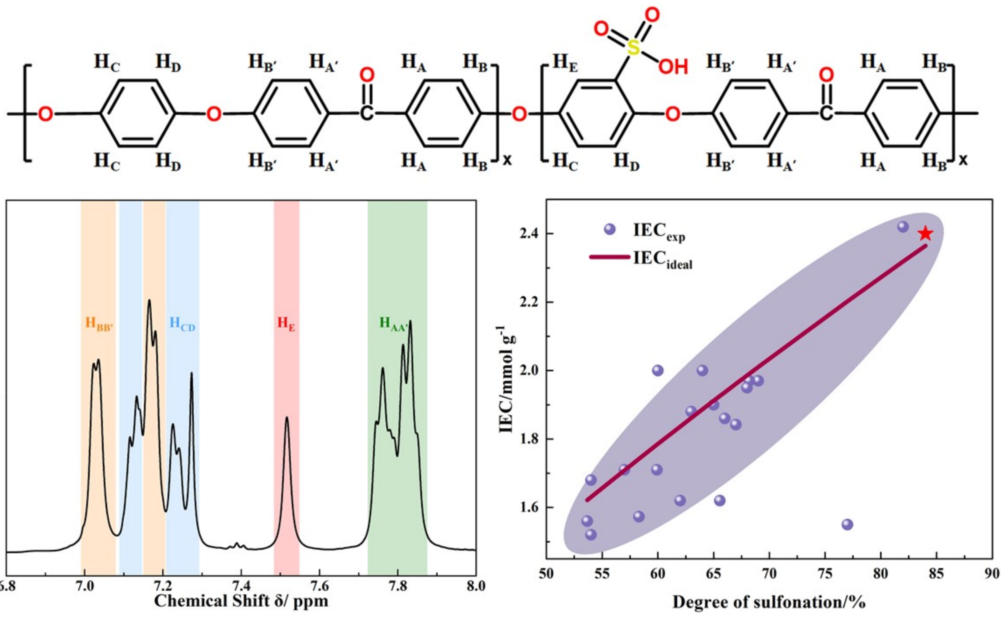

Figure S5 [1]H-NMR spectra of SPEEK; comparison between the IEC values measured in the literature at different DS and the theoretical IEC values

Note: The degree of sulfonation (DS) of SPEEK can be calculated from the liquid NMR peak area:

$$\frac{\mathbf{n}}{(\mathbf{12}-\mathbf{2n})}=\frac{A_{H_E}}{\sum A_{H_{AA'BB'CD}}}$$

$$\mathbf{DS}=\mathbf{n}\times\mathbf{100\%}$$

where n is the number of per repeat unit, A_{H_E} and $A_{H_{AA'BB'CD}}$ are the integral peak areas of H_E signals and signals corresponding to all other aromatic hydrogens, respectively.

The DS of SPEEK can also be calculated by IEC (10.1016/j.jpowsour.2013.03.016):

$$\mathbf{DS}(\%)=\frac{\mathbf{288}\times\mathbf{IEC}}{\mathbf{1000}-\mathbf{80}\times\mathbf{IEC}}\times\mathbf{100\%}$$

where 288 is the molar mass of PEEK (g mol^{-1}), 80 is the molar mass of -SO_3H (g mol^{-1}), and 1000 is the calculation factor when the units of other values are the same as above. The theoretical IEC value can be obtained from DS by the above equation. Comparing the IEC values measured in the literature at different DS with the theoretical IEC values, it can be found that DS and IEC satisfy the above equation very well, and the data we measured should be accurate accordingly.

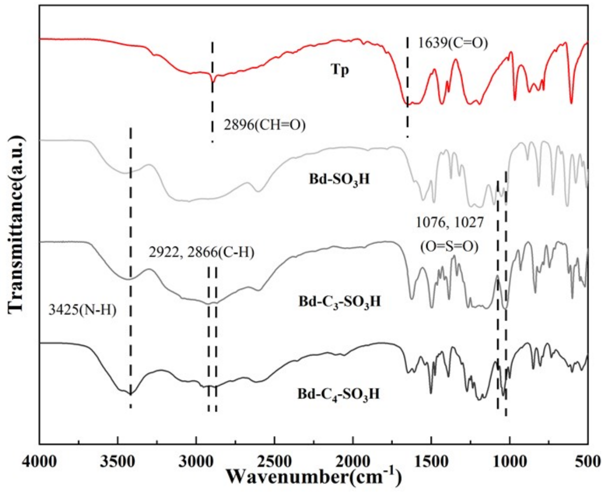

Figure S6 FTIR spectra of monomers

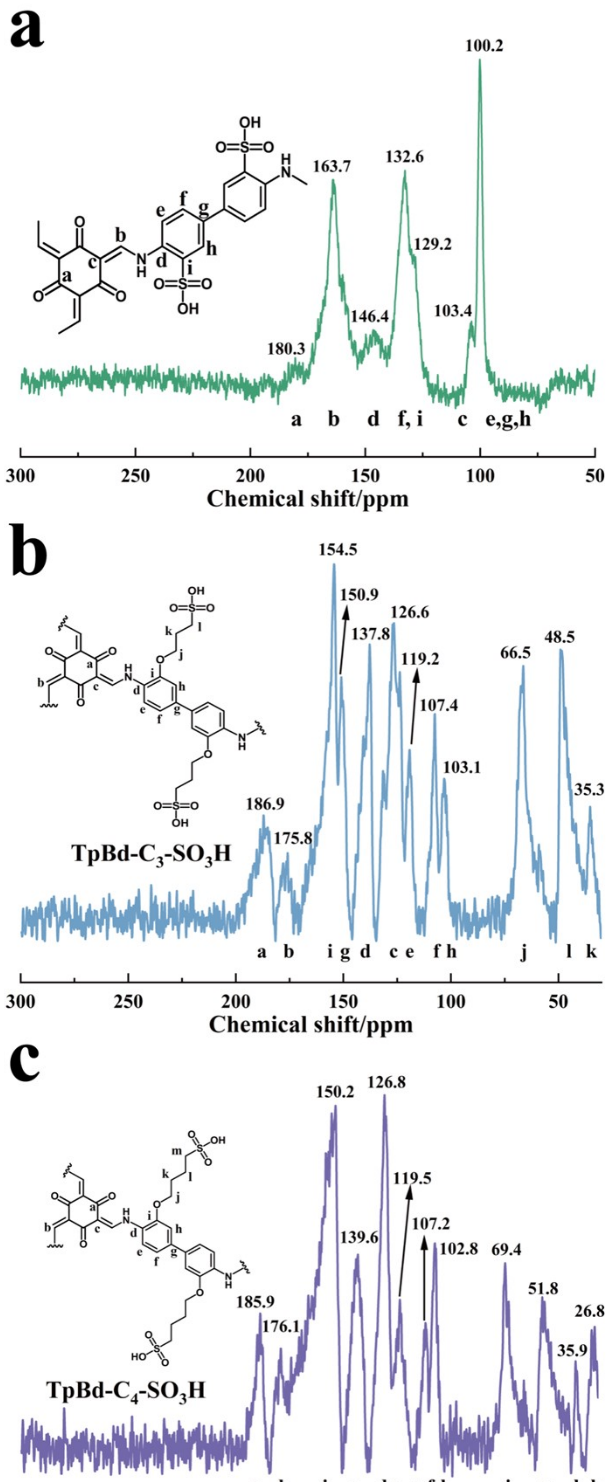

Figure S7 ^{13}C-NMR spectr of iCOFs

(a) TpBd-SO$_3$H; (b) TpBd-C$_3$-SO$_3$H; (c) TpBd-C$_4$-SO$_3$H

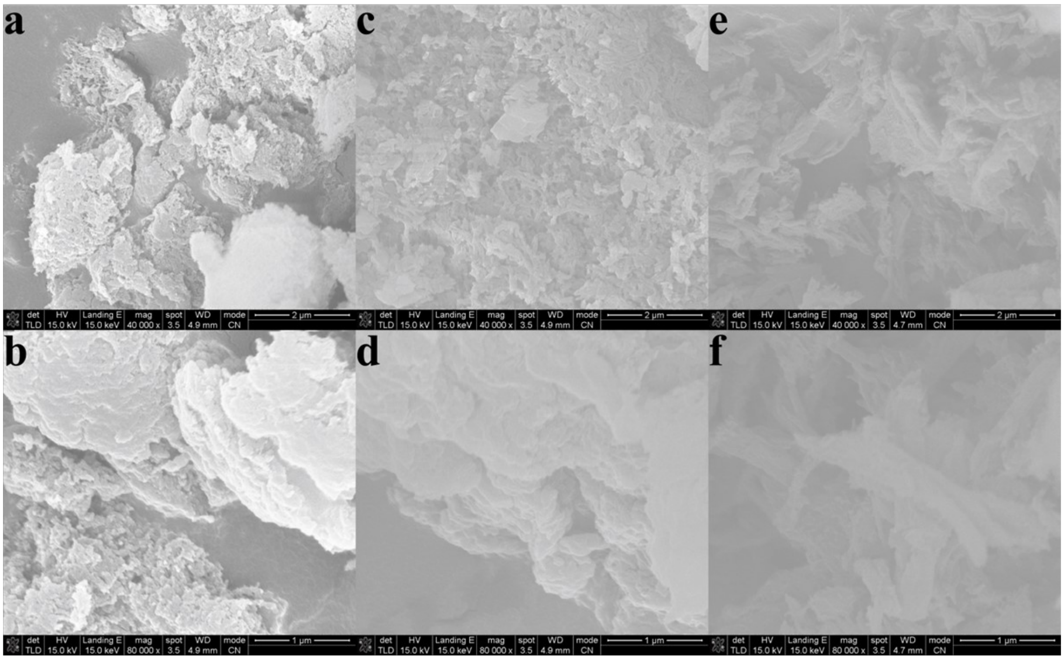

Figure S8 SEM images of iCOFs

(a, b) TpBd-SO_3H; (c, d) TpBd-C_3-SO_3H; (e, f) TpBd-C_4-SO_3H

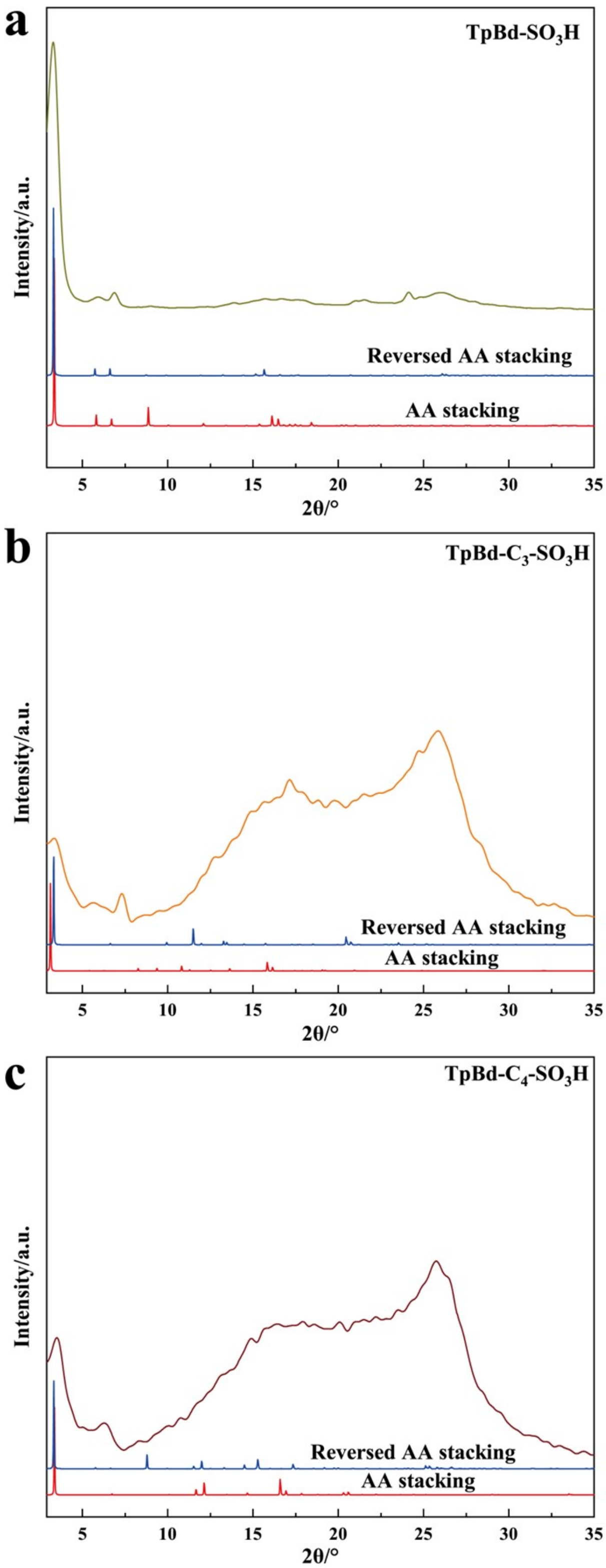

Figure S9 The XRD patterns of the TpBd-SO$_3$H, TpBd-C$_3$-SO$_3$H, and TpBd-C$_4$-SO$_3$H and the simulation results.

Table S1 Detailed atom information of the simulated TpBd-C_4-SO_3H in reversed AA Stacking

a=b=30.7388Å, c=7.0836Å; alpha=beta=90°, gamma = 120°; P6/M space group

Atoms	x	y	z	Atoms	x	y	z
O1	0.73631	0.92895	0.80739	H41	0.5833	0.89089	0.2395
H2	0.58887	0.92992	0.43306	H42	0.5476	0.84351	0.6249
H3	0.57065	0.82315	0.43932	H43	0.63367	0.91638	0.69255
H4	0.63014	0.85796	0.72369	H44	0.67826	0.86708	0.44257
H5	0.67178	0.91767	0.35603	N45	0.41515	0.81166	0.433
N6	0.57961	0.18883	0.44591	C46	0.36659	0.77275	0.4407
C7	0.62881	0.22643	0.44951	C47	0.35098	0.72019	0.4407
C8	0.64671	0.27944	0.45017	C48	0.38497	0.7013	0.44099
C9	0.61462	0.30054	0.45059	O49	0.2655	0.70071	0.44253
O10	0.73086	0.29487	0.45179	H50	0.44025	0.80119	0.42163
H11	0.55529	0.20046	0.43965	H51	0.33893	0.7821	0.44529
H12	0.65535	0.21558	0.4504	C52	0.40766	0.88764	0.47574
C13	0.5846	0.11137	0.47851	C53	0.43101	0.94072	0.48222
C14	0.55995	0.05824	0.48176	C54	0.48298	0.97301	0.44332
C15	0.50753	0.02715	0.44816	C55	0.50948	0.94757	0.39787
C16	0.4813	0.05376	0.41934	C56	0.48744	0.8945	0.39974
C17	0.50515	0.10707	0.42314	C57	0.43511	0.86303	0.43546
C18	0.55808	0.13731	0.44747	H58	0.37017	0.86704	0.50416
H19	0.62237	0.13101	0.50142	H59	0.40892	0.95558	0.51829
H20	0.58158	0.04251	0.51144	H60	0.54602	0.96814	0.35808
H21	0.44376	0.03426	0.39294	O61	0.47819	0.13138	0.4084
O22	0.51559	0.87189	0.36727	C62	0.42636	0.11263	0.45315
C23	0.5688	0.89135	0.38024	C63	0.41648	0.1569	0.43093
C24	0.57697	0.8567	0.51634	C64	0.37212	0.1524	0.55338
C25	0.6292	0.88322	0.61668	S65	0.30329	0.05187	0.65911
S26	0.73313	0.94434	0.59588	O66	0.32645	0.01639	0.57475
O27	0.73819	1.00143	0.59429	C67	0.31938	0.1059	0.5114
C28	0.67504	0.89961	0.48357	H68	0.29842	-0.00912	0.50004
H29	0.76403	1.01922	0.497	O69	0.0182	0.23981	1.11176
O30	0.32141	0.06742	0.87086	H70	0.08586	0.40465	0.94502
H31	0.41957	0.09894	0.59884	H71	0.19326	0.45433	1.09276
H32	0.41064	0.16047	0.28068	H72	0.15134	0.37271	1.25678
H33	0.36986	0.18648	0.53243	H73	0.12046	0.29364	1.01943
H34	0.31596	0.09421	0.36396	O74	0.95206	0.7781	0.95589
O35	0.24425	0.01623	0.66152	H75	0.92028	0.58758	0.95433
H36	0.40177	0.08169	0.35918	H76	0.82588	0.55289	1.19403
H37	0.45099	0.19142	0.47118	H77	0.89744	0.6422	1.27556
H38	0.38125	0.1524	0.70283	H78	0.87455	0.67935	0.91059
H39	0.29037	0.1158	0.53842	O79	0.93034	0.74359	1.30017
O40	0.77905	0.94928	0.47693	H80	0.91624	0.57432	1.20111

H81	0.83208	0.57058	0.95546	C125	0.1373	0.55888	0.94322
H82	0.84152	0.63891	1.19946	H126	0.13006	0.62225	0.88197
H83	0.9227	0.66408	0.90326	H127	0.04138	0.58036	0.87355
O84	0.06504	0.30232	1.37935	H128	0.03526	0.44436	1.01251
H85	0.10068	0.42105	1.18814	O129	0.87175	0.51355	1.0288
H86	0.17113	0.42626	0.87135	C130	0.89483	0.56602	1.06946
H87	0.18985	0.37202	1.07576	C131	0.85258	0.57881	1.08915
H88	0.10148	0.32809	0.87636	C132	0.87287	0.63431	1.15261
N89	0.81172	0.41366	0.95586	S133	0.94567	0.73496	1.09513
C90	0.77249	0.36527	0.94963	O134	1.00235	0.73935	1.1086
C91	0.72007	0.35032	0.9501	C135	0.90132	0.67453	0.99701
C92	0.70178	0.38482	0.95017	H136	1.02106	0.76371	1.00812
O93	0.69952	0.26459	0.95041				
H94	0.80145	0.43896	0.96526				
H95	0.7815	0.33735	0.94594				
C96	0.88794	0.40618	0.91516				
C97	0.94111	0.42978	0.91156				
C98	0.97309	0.48182	0.95061				
C99	0.94734	0.508	0.99562				
C100	0.89427	0.4855	0.99377				
C101	0.86302	0.43338	0.95498				
H102	0.86745	0.36874	0.88555				
H103	0.95627	0.40785	0.87678				
H104	0.96771	0.54479	1.03305				
O105	0.13316	0.48071	0.99926				
C106	0.11537	0.42919	1.0439				
C107	0.16158	0.42251	1.02169				
C108	0.15498	0.37241	1.10309				
S109	0.05322	0.29744	1.15987				
O110	0.01852	0.32449	1.11244				
C111	0.11026	0.32299	1.02129				
H112	0.00746	0.30049	1.02656				
N113	0.18883	0.58072	0.94443				
C114	0.22653	0.6298	0.9407				
C115	0.27951	0.64721	0.94144				
C116	0.30016	0.61471	0.94177				
O117	0.29571	0.73154	0.94198				
H118	0.20049	0.55644	0.95196				
H119	0.21585	0.65649	0.93874				
C120	0.11078	0.58464	0.90861				
C121	0.05763	0.55934	0.90678				
C122	0.02719	0.50708	0.9463				
C123	0.05438	0.48171	0.98156				
C124	0.10768	0.50626	0.97632				

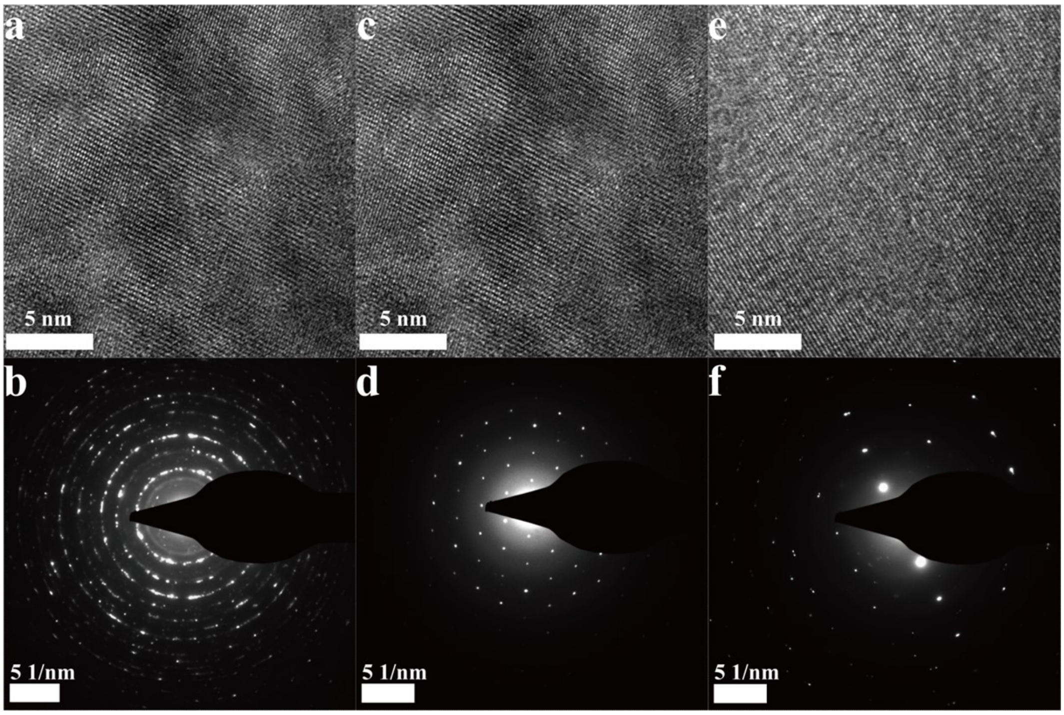

Figure S10 TEM images and SAED images of iCOFs

(a, b) TpBd-SO_3H; (c, d) TpBd-C_3-SO_3H; (e, f) TpBd-C_4-SO_3H

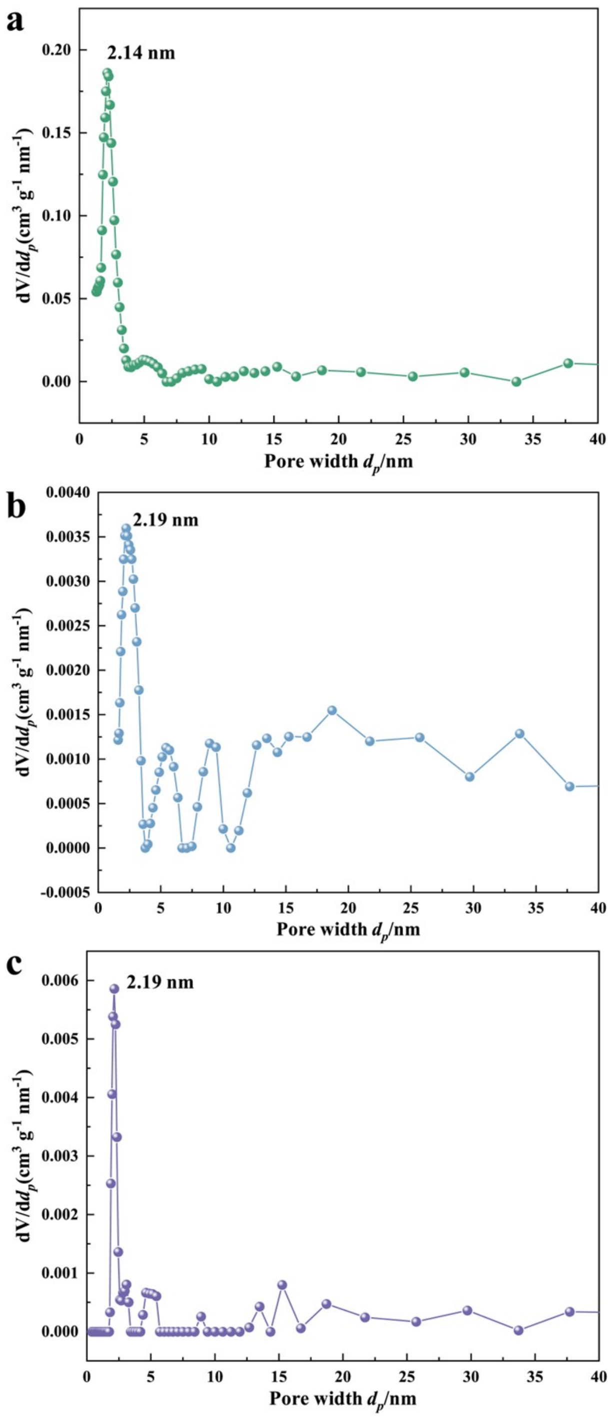

Figure S11 Pore size distribution (PSDs) of TpBd-C_x-SO_3H iCOFs

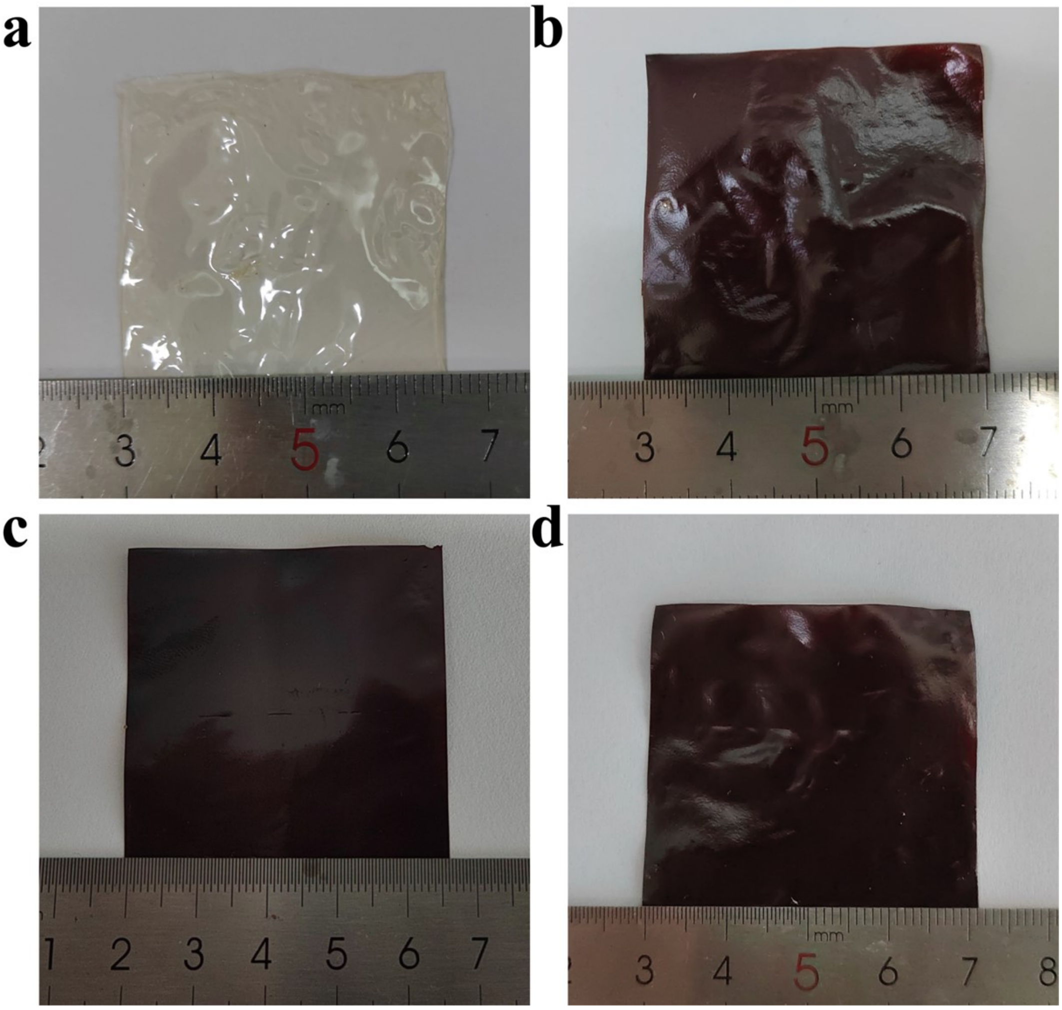

Figure S12 Digital photo pf (a)SPEEK, (b)SPEEK/TpBd-SO_3H-6, (c)SPEEK/TpBd-C_3-SO_3H-6, (d)SPEEK/TpBd-C_4-SO_3H-6,

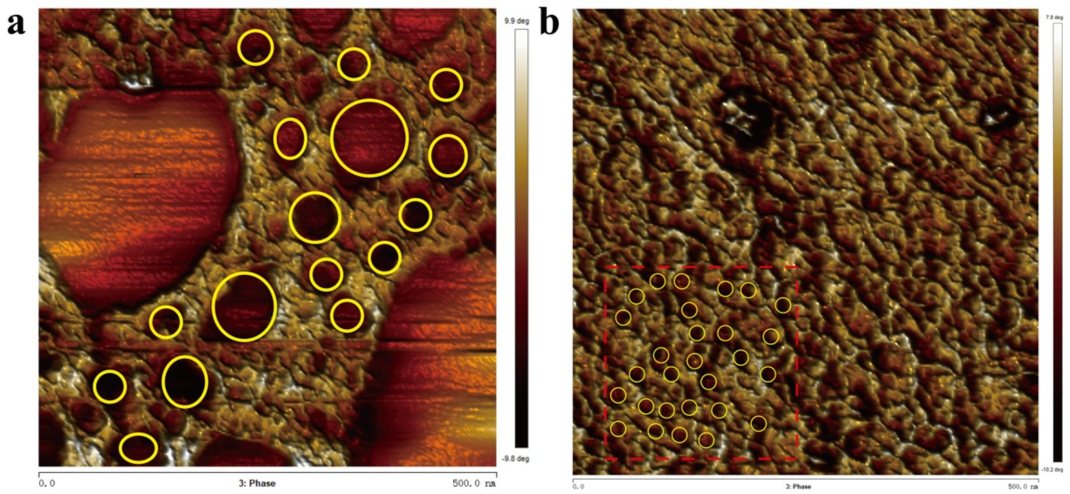

Figure S13 AFM phase image of (a)SPEEK, (b)SPEEK/TpBd-C_3-SO_3H-6. The regions with the yellow circle are soft and the bright regions are hard.

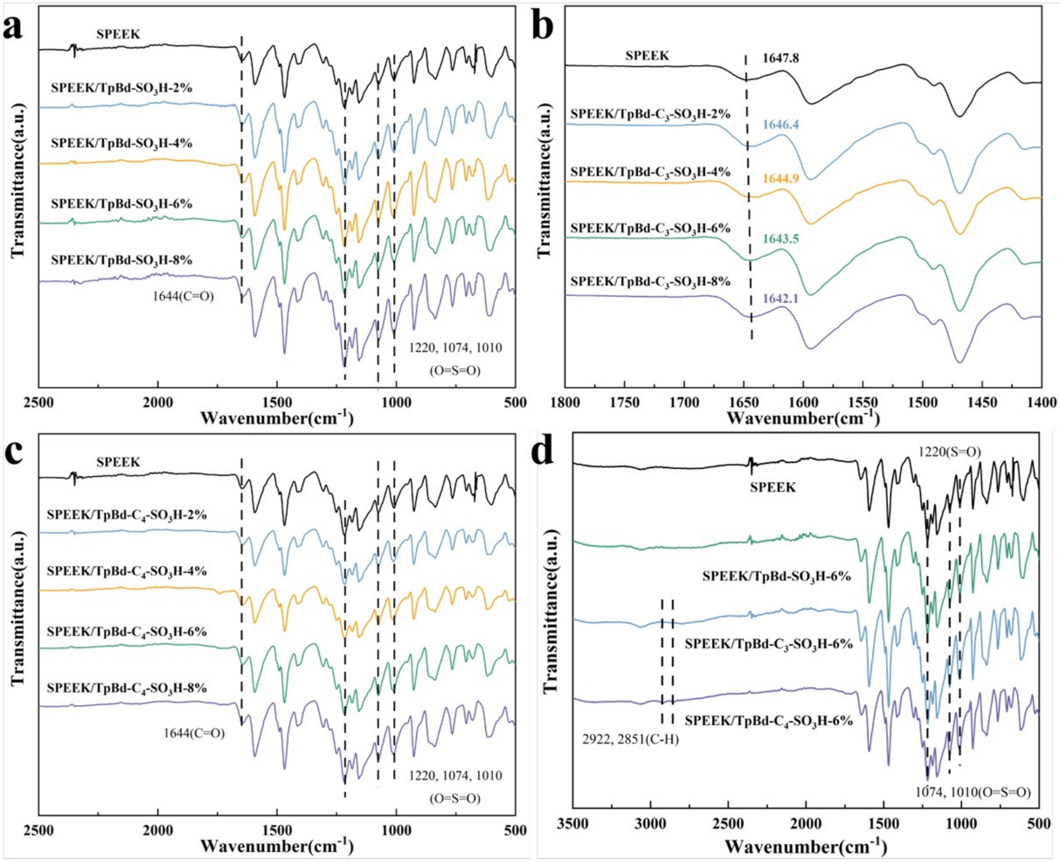

Figure S14 FTIR spectra of SPEEK/TpBd-C_x-SO_3H-y membranes (a) SPEEK/TpBd-SO_3H; (b) SPEEK/TpBd-C_3-SO_3H; (c) SPEEK/TpBd-C_4-SO_3H; (d) SPEEK/TpBd-C_x-SO_3H-6

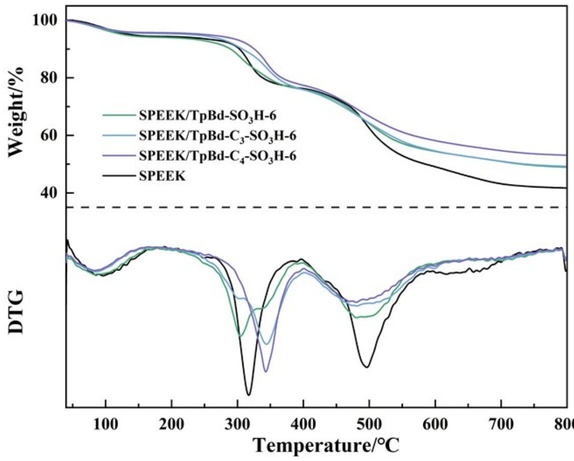

Figure S15 TGA curves and DTG curves of SPEEK and SPEEK/TpBd-C_x-SO_3H-6

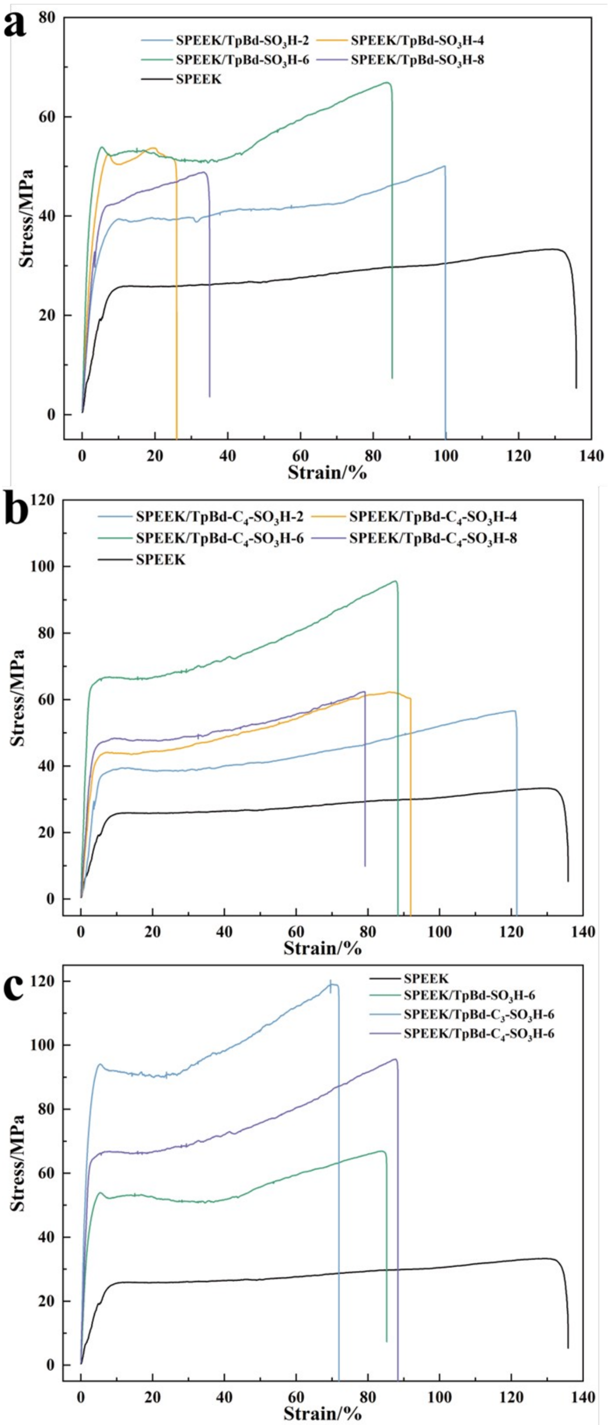

Figure S16 Stress-strain curves of SPEEK/TpBd-C_x-SO_3H-y

Table S2 Mechanical strength and strain rate of SPEEK/TpBd-C_x-SO_3H-y

Sample	Mechanical Strength (MPa)	Elongation at break/%
SPEEK	33.33	129.05
SPEEK/TpBd-SO_3H-2	50.07	99.70
SPEEK/TpBd-SO_3H-4	53.74	19.35
SPEEK/TpBd-SO_3H-6	66.91	83.73
SPEEK/TpBd-SO_3H-8	48.88	33.19
SPEEK/TpBd-C_3-SO_3H-2	93.18	88.25
SPEEK/TpBd-C_3-SO_3H-4	101.87	76.20
SPEEK/TpBd-C_3-SO_3H-6	120.41	69.62
SPEEK/TpBd-C_3-SO_3H-8	73.85	16.66
SPEEK/TpBd-C_4-SO_3H-2	56.59	120.24
SPEEK/TpBd-C_4-SO_3H-4	62.30	85.92
SPEEK/TpBd-C_4-SO_3H-6	95.65	87.57
SPEEK/TpBd-C_4.SO_3H-8	62.39	79.05

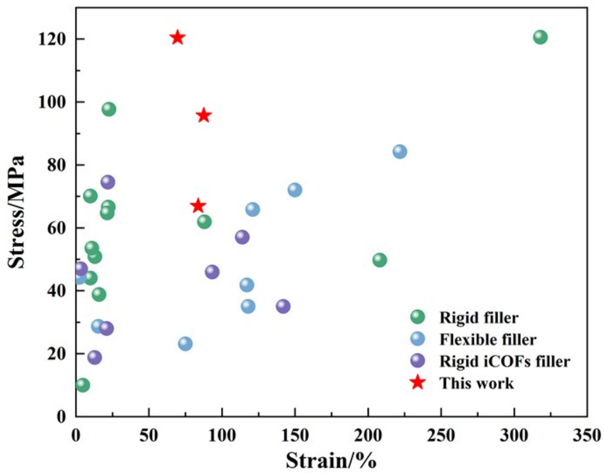

Figure S17 Comparison of the mechanical stability and strain rate between SPEEK/TpBd-C_3-SO_3H-6 and hybrid PEMs reported in the literature

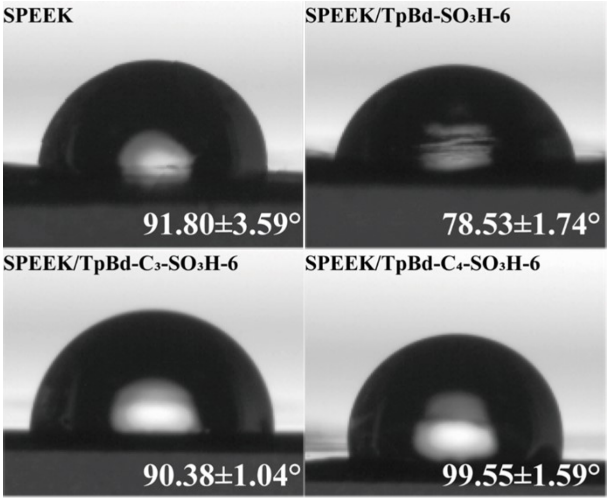

Figure S18 Water contact angle of SPEEK and SPEEK/TpBd-C_x-SO_3H-6

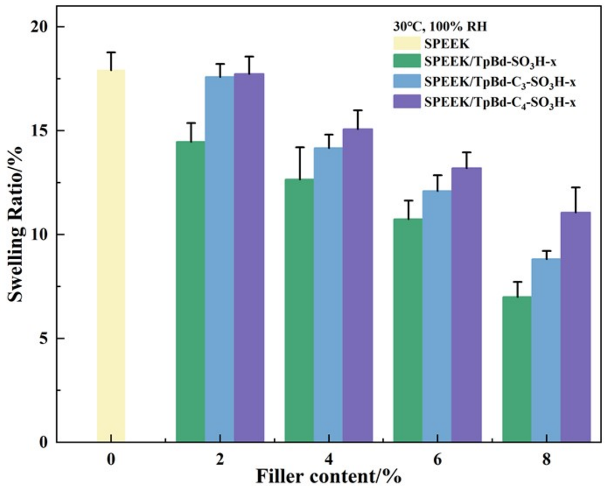

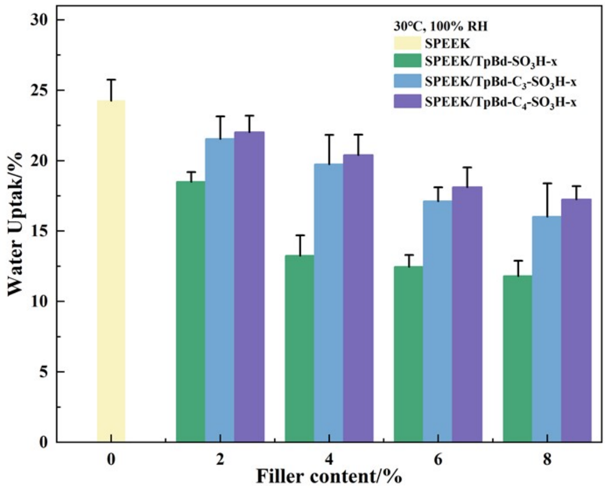

Figure S19 Water uptake and swelling ratio of SPEEK/TpBd-C_x-SO_3H-y at 30°C, 100% RH

Table S3 Water uptake and swelling ratio of SPEEK/TpBd-C_x-SO_3H-y

Sample	30℃		60℃	
	WU/%	SR/%	WU/%	SR/%
SPEEK	24.3±1.5	17.9±0.9	69.4±1.7	45.2±3.0
SPEEK/TpBd-SO_3H-2	18.5±0.7	14.5±0.9	31.6±2.6	26.2±3.5
SPEEK/TpBd-SO_3H-4	13.3±1.4	12.7±1.5	26.4±1.8	23.3±3.3
SPEEK/TpBd-SO_3H-6	12.5±0.8	10.7±0.9	24.7±2.3	22.5±1.7
SPEEK/TpBd-SO_3H-8	11.8±1.1	7.0±0.7	21.2±1.9	14.7±3.4
SPEEK/TpBd-C_3-SO_3H-2	21.5±1.6	17.6±0.6	33.8±1.2	27.5±0.6
SPEEK/TpBd-C_3-SO_3H-4	19.7±2.1	14.2±0.6	28.7±1.3	24.7±2.8
SPEEK/TpBd-C_3-SO_3H-6	17.1±1.0	12.1±0.8	25.3±1.4	23.2±1.9
SPEEK/TpBd-C_3-SO_3H-8	16.0±2.4	8.8±0.4	23.7±2.1	18.1±1.8
SPEEK/TpBd-C_4-SO_3H-2	22.0±1.2	17.7±0.8	35.2±1.3	35.1±3.2
SPEEK/TpBd-C_4-SO_3H-4	20.4±1.4	15.1±0.9	31.7±2.7	33.2±2.5
SPEEK/TpBd-C_4-SO_3H-6	18.1±1.4	13.2±0.8	29.2±1.9	28.8±2.5
SPEEK/TpBd-C_4.SO_3H-8	17.2±0.9	11.1±1.2	28.5±3.6	24.6±3.2

Table S4 Comparison of the theoretical IEC and experimental IEC

Sample	IEC_{exp} (mmol g^{-1})	IEC_{ideal} (mmol g^{-1})
SPEEK/TpBd-SO_3H-2	2.521±0.040	2.443
SPEEK/TpBd-SO_3H-4	2.546±0.042	2.482
SPEEK/TpBd-SO_3H-6	2.611±0.039	2.519
SPEEK/TpBd-SO_3H-8	2.546±0.038	2.555
SPEEK/TpBd-C_3-SO_3H-2	2.438±0.035	2.425
SPEEK/TpBd-C_3-SO_3H-4	2.475±0.035	2.447
SPEEK/TpBd-C_3-SO_3H-6	2.515±0.037	2.467
SPEEK/TpBd-C_3-SO_3H-8	2.445±0.038	2.487
SPEEK/TpBd-C_4-SO_3H-2	2.410±0.051	2.422
SPEEK/TpBd-C_4-SO_3H-4	2.431±0.039	2.440
SPEEK/TpBd-C_4-SO_3H-6	2.466±0.034	2.458
SPEEK/TpBd-C_4.SO_3H-8	2.425±0.037	2.475

Note:

The theoretical IEC of iCOF can be calculated based on the chemical structure and molecular weight of the monomer.

Aldehyde monomer Tp and amine monomer Bd-C_x-SO_3H undergo Schiff base reaction polymerization and dehydration to obtain iCOF, and the two react in a molar ratio of 2:3, so it is assumed that the aldehyde group and the amino group in two Tp molecules and three Bd-C_x-SO_3H molecules are all involved in the reaction, and from this, the experimental relative molecular weights of the polymers can be calculated (taking TpBd-C_3-SO_3H as an example) :

$$\begin{aligned} M_{TpBd-C_3-SO_3H} &= 2M_{Tp} + 3M_{Bd-C_3-SO_3H} - 6M_{H_2O} \\ &= 2\times 210.14 + 3\times 460.10 - 6\times 18.01 \\ &= 1692.52 \end{aligned}$$

Based on this experimental formula, six -SO_3H groups exist within iCOF, from which the theoretical IEC of iCOF can be calculated:

$$IEC_{TpBd-C_3-SO_3H} = \frac{n(-SO_3H)}{M_{TpBd-C_3-SO_3H}/1000} = \frac{6}{1692.52/1000} = 3.54\ \text{mmol g}^{-1}$$

From this, the theoretical IEC of the three iCOFs were calculated as TpBd-SO_3H (4.46 mmol g^{-1})，TpBd-C_3-SO_3H (3.54 mmol g^{-1})，TpBd-C_4-SO_3H (3.37 mmol g^{-1}).

Based on the mass ratio of SPEEK to iCOF can be further calculated to obtain the theoretical IEC of the hybrid matrix membrane (SPEEK/TpBd-C_3-SO_3H-6 as an example):

$$\begin{aligned} IEC_{membrane} &= \frac{IEC_{SPEEK}\times m_{SPEEK} + IEC_{TpBd-C_3-SO_3H}\times m_{TpBd-C_3-SO_3H}}{m_{SPEEK} + m_{TpBd-C_3-SO_3H}} \\ &= \frac{2.403\times 200 + 3.54\times 12}{200+12} = 2.467\ \text{mmol g}^{-1} \end{aligned}$$

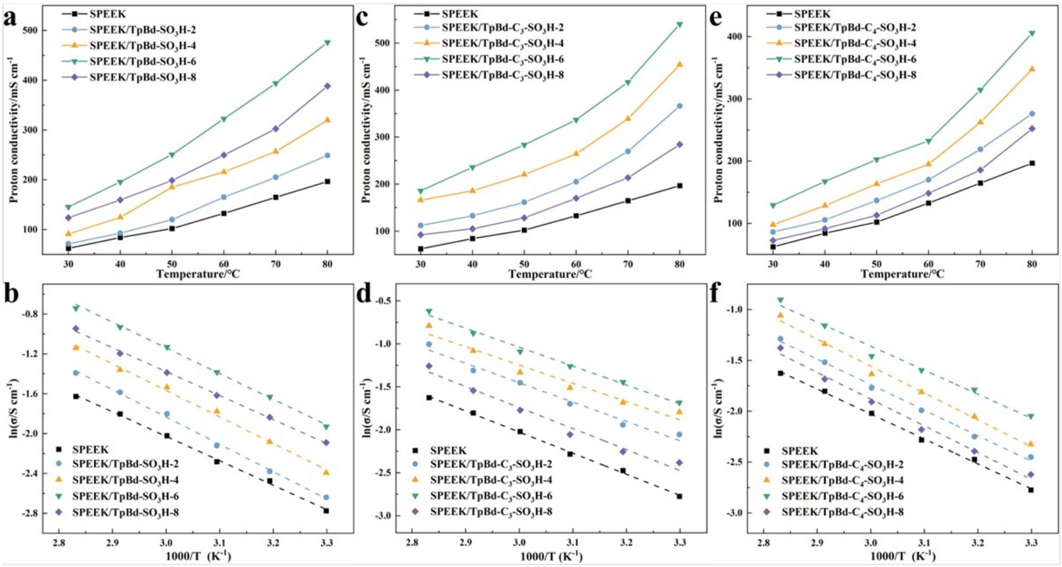

Figure S20 Temperature-dependent proton conductivity curves of and Arrhenius plots of SPEEK/TpBd-C_x-SO_3H-y

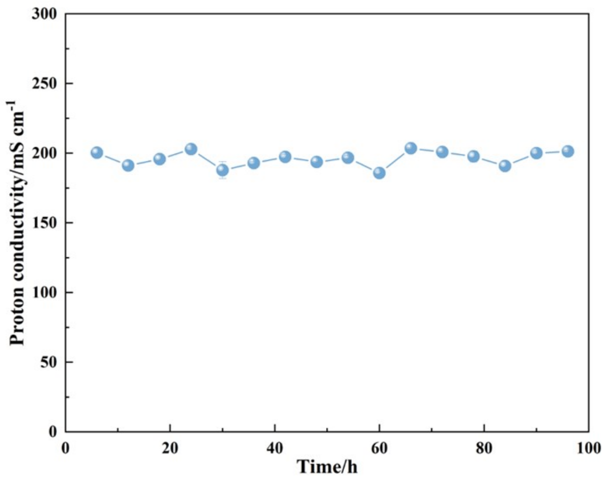

Figure S21 Time-dependent conductivity of SPEEK/TpBd-C_3-SO_3H-6 at 30℃ 100%RH.

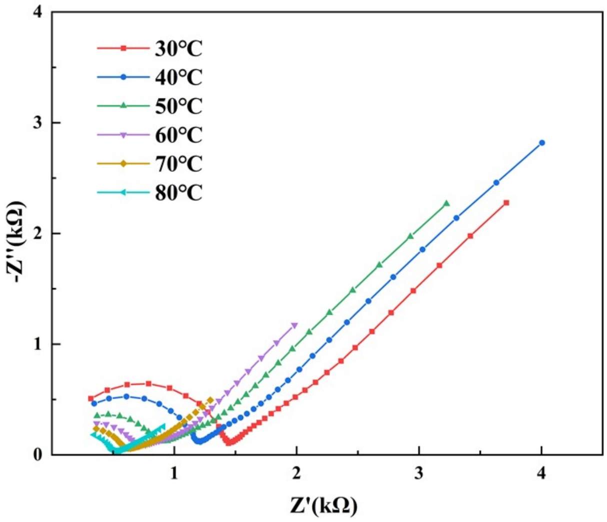

Figure S22 Nyquist plots of SPEEK/TpBd-C_3-SO_3H-6 membrane under 100%RH at different temperatures.

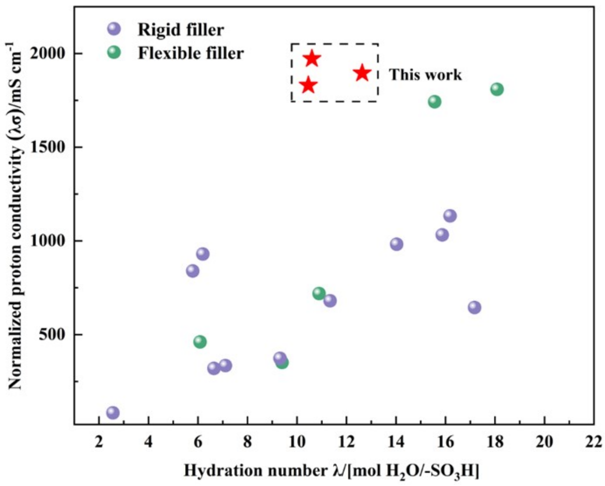

Figure S23 Comparison of normalized proton conductivity (30°C 100%RH) with hydration numeber between SPEEK/TpBd-C_3-SO_3H-6 and hybrid PEMs reported in the literature.

Note: The hydration numeber (λ) was defined the number of water molecules adsorbed by cationic group, which was calculated according to the following:

$$\lambda = \frac{\mathbf{Wu} \times \mathbf{10}}{\mathbf{IEC} \times \mathbf{18}}$$

where Wu was obtained in deionized water at 30°C.

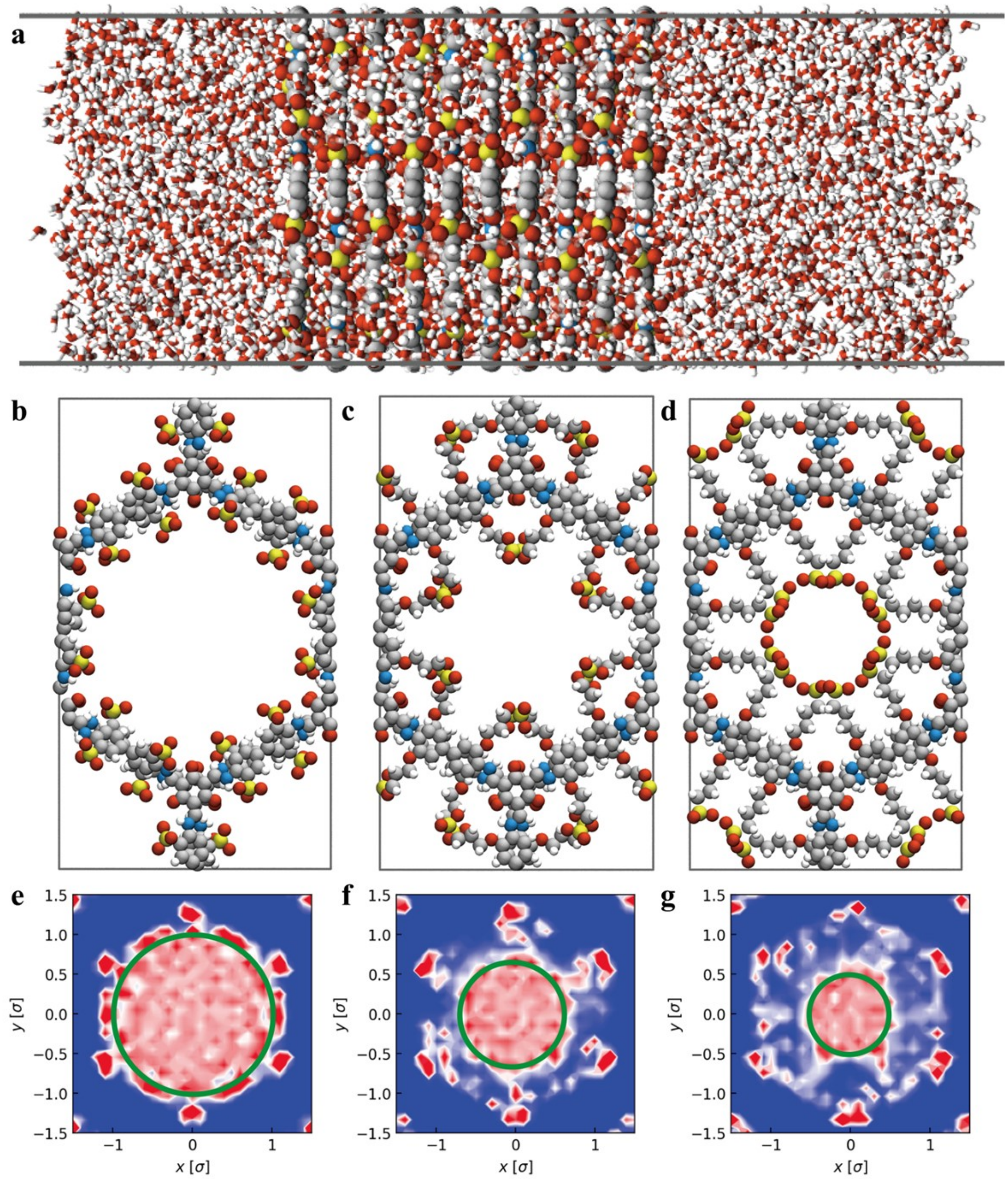

Figure S24 Distribution of water molecules of 3500 H_2O plus 120 H_3O^+ in (a) ten stacked (Reversed AA stacking) (b, e) TpBd-SO_3H, (c, f) TpBd-C_3-SO_3H, and (d, g) TpBd-C_4-SO_3H nanosheets.

Note: The "local" refers to the region of high-density water molecule distribution around the sulfonic acid groups in iCOF channel (the region shown in the green circle range). Due to the introduction of the side chains, the -SO3H groups tend to aggregate into clusters. For TpBd-C_3-SO_3H and TpBd-C_4-SO_3H, the range of its ionic clusters is the "local" region.

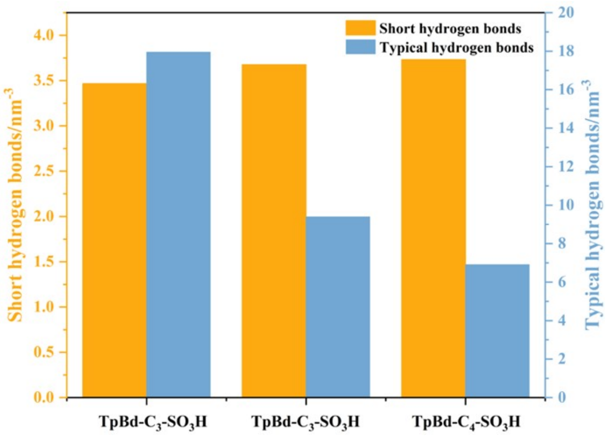

Figure S25 Density of hydrogen bonds in iCOF channel

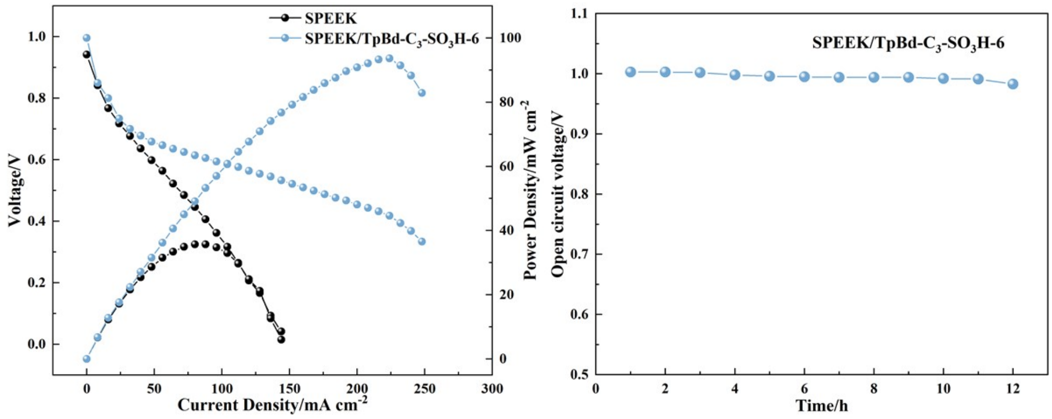

Figure S26 Single PEMFC performances of SPEEK and SPEEK/TpBd-C_3-SO_3H-6; Open circuit voltage of SPEEK/TpBd-C_3-SO_3H-6 at 25°C, 100% RH.

Note:

The catalyst (Pt/C = 40%), Nafion solution, isopropyl alcohol, and deionized water were mixed in proportion. The catalyst ink was obtained by ultrasonication for 1 h, and then was uniformly painted on a certain area of hybrid PEMs to make Pt loading density of 0.5 mg cm^{-2}. The front and back sides of the membrane sample were painted with catalyst to prepare membrane-electrode assembly (MEA). Then the MEA was sealed between the two plates of a single battery and tested using the NTT-PEM-25W system. The single PEMFC (H_2/O_2) performance was detected by humidified H_2 and O_2 (both 100 mL min^{-1}) at 25 °C and 100% RH.

Table S5 IEC, σ (80°C, 100% RH), and activation energy (Ea) of the membranes

Sample	**IEC (mmol g^{-1})**	**σ (mS cm^{-1})**	**Ea (eV)**
SPEEK	2.403±0.039	196.6±0.5	0.21
SPEEK/TpBd-SO_3H-2	2.521±0.040	249.9±3.1	0.24
SPEEK/TpBd-SO_3H-4	2.546±0.042	320.2±4.8	0.23
SPEEK/TpBd-SO_3H-6	2.611±0.039	476.1±7.7	0.22
SPEEK/TpBd-SO_3H-8	2.546±0.038	349.5±4.5	0.21
SPEEK/TpBd-C_3-SO_3H-2	2.438±0.035	366.2±0.7	0.20
SPEEK/TpBd-C_3-SO_3H-4	2.475±0.035	454.0±4.3	0.19
SPEEK/TpBd-C_3-SO_3H-6	2.515±0.037	540.4±3.3	0.18
SPEEK/TpBd-C_3-SO_3H-8	2.445±0.038	284.4±4.8	0.25
SPEEK/TpBd-C_4-SO_3H-2	2.410±0.051	276.2±3.7	0.22
SPEEK/TpBd-C_4-SO_3H-4	2.431±0.039	347.6±5.3	0.23
SPEEK/TpBd-C_4-SO_3H-6	2.466±0.034	406.0±0.4	0.20
SPEEK/TpBd-C_4-SO_3H-8	2.425±0.037	252.3±0.9	0.25

Table S6 Comparison of proton conductivity and mechanical strength for polymer-based hybrid membranes in the literature and in this work.

Membranes	IEC (mmol g^{-1})	Mechanical Strength (MPa)	Testing condition	σ (mS cm^{-1})	Ref
SPEEK/HPW@mGO-4	1.51	70.1	75℃ 100%RH	180	[1]
SPEEK/PAPOP-4%	1.794	120.6	80℃ 100%RH	417.0	[2]
SPEEK/ZCN-2.5	1.48	50.8	70℃ 95%RH	206	[3]
SPEEK/S-UiO-66@GO-10	1.7	53.5	70℃ 95%RH	268	[4]
C-SPEEK/HPW/GO	1.45	38.77	80℃ 100%RH	119.04	[5]
Zeolite 4A (4 wt.%)-SPEEK-MSA (20 wt.%)	1.75	10	70℃ 100%RH	137	[6]
IL@MIL-125-NH2/SPEEK-5	1.71	59.81	65℃ 100%RH	320	[7]
S/PA@FT2	1.98	44	80℃ 100%RH	128	[8]
SP-ZIF-L@GO-5	1.51	66.6	70℃ 100%RH	265	[9]
SPEEK/MoS2@CNTs-1	1.52	64.7	80℃ 100%RH	131	[10]
SPEEK/SO3H-UGNF (1 wt%)	1.7	97.7	90℃ 100%RH	161.2	[11]
SPEEK/UNCS-3	1.3	61.9	75℃ 100%RH	186.4	[12]
SSiO2_1/ZIF-C-SO_3H_3@SPEEK	1.67	49.7	60℃ 100%RH	164.9	[13]
SPP68-FSS2.5	1.7	68	90℃ 98%RH	127	[14]
SPAES-2CST3	1.41	52.9	80℃ 100%RH	128.1	[15]
HPWILs @MOF-4	0.97	40.6	100℃ 100%RH	138	[16]
QPPO/F-p-gC3N4-0.5	1.42	17	90℃ 100%RH	142.1	[17]
3% SPES-MOF	0.85	22.41	80℃ 100%RH	214.8	[18]
GSiW11-Nf-3%	0.87	12.6	80℃ 100%RH	226	[19]
Nafion-Bi12-3%	0.95	14.6	80℃ 100%RH	132	[20]
SPI-Fe@MOF-1%	1.65	105	80℃ 100%RH	192	[21]
4NP-SPEEK-4NP	1.46	65.8	60℃ 100%RH	162	[22]
SPGP2-4	0.84	28.7	80℃ 100%RH	126.8	[23]
S-$DMEA_{30}$-BPT/PA	1.81	84.2	80℃ 100%RH	295.4	[24]
HQ/ALE/PEI-PTFE@SPEEK70	1.53	23.13	80℃ 100%RH	210	[25]
t-SPEEK/SPAES(1:2:1)	1.72	35	80℃ 100%RH	181.2	[26]
SP@PQD-15.1	1.69	73.2	80℃ 100%RH	138.2	[27]
1.5%PI/SPEEK/1.5%PI	1.533	41.8	60℃ 100%RH	177.9	[28]
SPEEK/QNPAES (6 wt%)	2.1	44.2	90℃ 100%RH	136	[29]
PPCDM-50	2.42	56	80℃ 100%RH	264	[30]
SPEEK-C50/PA	1.88	72	80℃ 100%RH	270	[31]
SP-BNP-10	1.46	62	75℃ 100%RH	103	[32]
F-CQPAEK@Nafion-1.0	0.92	18.55	80℃ 100%RH	211	[33]

SPEEK-IM/CSPF-10	1.78	95	90℃ 100%RH	81.45	[34]
SPEEK/H3PO4@CTFp-15	1.47	47.0	80℃ 100%RH	313	[35]
Nafion/Z-COF-10	0.85	28	80℃ 100%RH	220	[36]
QA@COF-LZU1/PPO-5	2.72	18.8	80℃ 100%RH	168	[37]
SPEEK/S-SNW-15	2.11	45.98	80℃ 100%RH	115.53	[38]
SPEEK/TpPa-SO_3H-20	2.26	35	60℃ 95%RH	443.6	[39]
MIM-SO_3H	1.8	57	80℃ 100%RH	88	[40]
SPEEK/TpPa-SO_3H-5	2.34	74.5	80℃ 100%RH	346	[41]
SPEEK/TpBd-SO_3H-6	2.611	66.91	80℃ 100%RH	476.1	This work
SPEEK/TpBd-C_3-SO_3H-6	2.515	120.41	80℃ 100%RH	540.4	
SPEEK/TpBd-C_4-SO_3H-6	2.466	95.65	80℃ 100%RH	405.9	

1

References

1. Q. Peng, Y. Li, M. Qiu, B. Shi, X. He, C. Fan, X. Mao, H. Wu and Z. Jiang, *Industrial & Engineering Chemistry Research*, 2021, **60**, 4460-4470.
2. S. Wang, T. Zhu, B. Shi, C. Fan, Y. Liu, Z. Yin, Z. Gao, Z. Zhang, H. Wu and Z. Jiang, *Journal of Membrane Science*, 2023, **666**.
3. H. Sun, B. Tang and P. Wu, *ACS Appl Mater Interfaces*, 2017, **9**, 35075-35085.
4. H. Sun, B. Tang and P. Wu, *ACS Appl Mater Interfaces*, 2017, **9**, 26077-26087.
5. F. Sun, L.-L. Qin, J. Zhou, Y.-K. Wang, J.-Q. Rong, Y.-J. Chen, S. Ayaz, Y. U. Hai-Yin and L. Liu, *Journal of Membrane Science*, 2020, **611**.
6. S. Meenakshi, S. D. Bhat, A. K. Sahu, P. Sridhar and S. Pitchumani, *Fuel Cells*, 2013, DOI: 10.1002/fuce.201300022, n/a-n/a.
7. X. Wang, Y. Rong, F. Wang, C. Zhang and Q. Wang, *Microporous and Mesoporous Materials*, 2022, **346**.
8. P. Salarizadeh, M. Javanbakht, M. B. Askari, K. Hooshyari, M. Moradi, H. Beydaghi, M. Rastgoo-Deylami and M. Enhessari, *Sci Rep*, 2021, **11**, 4926.
9. Y. Y. Cai, Q. G. Zhang, A. M. Zhu and Q. L. Liu, *J Colloid Interface Sci*, 2021, **594**, 593-603.
10. F. Zhong, Z. Zeng, Y. Liu, R. Hou, X. Nie, Y. Jia, J. Xi, H. Liu, W. Niu and F. Zhang, *Polymer*, 2022, **249**.
11. A. R. Kim, M. Vinothkannan, S. Ramakrishnan, B.-H. Park, M.-K. Han and D. J. Yoo, *Applied Surface Science*, 2022, **593**.
12. J. Long, X. Zhang, S. Zeng, T. Pei, H. Ma, X. Li and X. Meng, *International Journal of Hydrogen Energy*, 2023, **48**, 2001-2012.
13. J. Li, W. Wang, Z. Jiang, B. Deng and Z.-j. Jiang, *Journal of Power Sources*, 2022, **543**.
14. K. Hooshyari, S. Heydari, H. Beydaghi and H. R. Rajabi, *Renewable Energy*, 2022, **186**, 115-125.
15. L. Liu, Y. Pu, Y. Lu, N. Li, Z. Hu and S. Chen, *Journal of Membrane Science*, 2021, **621**.
16. Z. Zhang, J. Ren, J. Xu, L. Meng, P. Zhao, H. Wang and Z. Wang, *Journal of Membrane Science*, 2021, **630**.
17. K. H. Lee, J. Y. Chu, A. R. Kim and D. J. Yoo, *Journal of Membrane Science*, 2022, **650**.
18. Y. Y. Xing, J. Wang, C. X. Zhang and Q. L. Wang, *ACS Appl Mater Interfaces*, 2023, **15**, 33003-33012.
19. H. He, Y. Zhu, T. Li, S. Song, L. Zhai, X. Li, L. Wu and H. Li, *ACS Nano*, 2022, **16**, 19240-19252.
20. B. Liu, B. Hu, J. Du, D. Cheng, H. Y. Zang, X. Ge, H. Tan, Y. Wang, X. Duan, Z. Jin, W. Zhang, Y. Li and Z. Su, *Angew Chem Int Ed Engl*, 2021, **60**, 6076-6085.
21. J. Yang, L. Tong, A. S. Alsubaie, K. H. Mahmoud, Y. Guo, L. Liu, L. Guo, Z. Sun and C. Wang, *Advanced Composites and Hybrid Materials*, 2022, **5**, 834-842.
22. D. Huang, X. Li, C. Luo, P. Wei, Y. Sui, J. Wen, C. Cong, X. Zhang, X. Meng

and Q. Zhou, *Journal of Membrane Science*, 2022, **662**.
23. G. Wang, J. Li, L. Zhai, X. Li, H. He, H. Guo, H. Li, C. Zhao, L. Wu and H. Li, *Composites Science and Technology*, 2023, **232**.
24. J. Wu, F. Wang, X. Fan, J. Chu, F. Cheng, F. Hu, H. Liu, Q. Zhang, Z. Xu and C. Gong, *Journal of Membrane Science*, 2023, **672**.
25. H. Park, V. D. C. Tinh and D. Kim, *Progress in Organic Coatings*, 2022, **163**.
26. A. Haragirimana, N. Li, Z. Hu and S. Chen, *International Journal of Hydrogen Energy*, 2021, **46**, 15866-15877.
27. Z. Zhou, Y. Wang, J. Lin, Y. Zhang, L. Qu, W. Wu and J. Wang, *International Journal of Hydrogen Energy*, 2021, **46**, 31312-31323.
28. P. Wei, Y. Sui, X. Li, Q. Liu, B. Zhu, C. Cong, X. Meng and Q. Zhou, *Journal of Membrane Science*, 2022, **644**.
29. A. R. Kim, M. B. Poudel, J. Y. Chu, M. Vinothkannan, R. Santhosh Kumar, N. Logeshwaran, B.-H. Park, M.-K. Han and D. J. Yoo, *Composites Part B: Engineering*, 2023, **254**.
30. B. Shi, X. Pang, H. Wu, J. Shen, J. Guan, X. Wang, C. Fan, L. Cao, T. Zhu, Z. Yin, Y. Kong, Y. Liu, S. Wang and Z. Jiang, *Journal of Materials Chemistry A*, 2022, **10**, 16995-17000.
31. J. Wu, S. Nie, H. Liu, C. Gong, Q. Zhang, Z. Xu and G. Liao, *Journal of Materials Chemistry A*, 2022, **10**, 19914-19924.
32. Q. Liu, X. Li, S. Zhang, Z. Wang, Y. Chen, S. Zhou, C. Wang, K. Wu, J. Liu, Q. Mao and X. Jian, *Journal of Membrane Science*, 2022, **641**.
33. Y. Duan, C. Ru, Y. Pang, J. Li, B. Liu and C. Zhao, *Journal of Membrane Science*, 2022, **655**.
34. P. Qian, L. Li, H. Wang, J. Sheng, Y. Zhou and H. Shi, *Journal of Membrane Science*, 2022, **662**.
35. X. Sun, J.-H. Song, H.-q. Ren, X.-y. Liu, X.-w. Qu, Y. Feng, Z.-Q. Jiang and H.-l. Ding, *Electrochimica Acta*, 2020, **331**.
36. Y. Li, H. Wu, Y. Yin, L. Cao, X. He, B. Shi, J. Li, M. Xu and Z. Jiang, *Journal of Membrane Science*, 2018, **568**, 1-9.
37. J. Chen, M. Guan, K. Li and S. Tang, *ACS Appl Mater Interfaces*, 2020, **12**, 15138-15144.
38. P. Li, N. Zhang, X. Li and S. Tang, *Green Energy & Environment*, 2023, **8**, 915-926.
39. X. Meng, Y. Lv, L. Ding, L. Peng, Q. Peng, C. Cong, H. Ye and Q. Zhou, *Nanomaterials (Basel)*, 2022, **12**.
40. R. Singh and D. Kim, *ACS Appl Mater Interfaces*, 2021, **13**, 33437-33448.
41. Z. Yin, H. Geng, P. Yang, B. Shi, C. Fan, Q. Peng, H. Wu and Z. Jiang, *International Journal of Hydrogen Energy*, 2021, **46**, 26550-26559.